Design and characterization of a wideband metamaterial absorber for microwave applications

Rachid Chaynane,[1,*], *Nawfal Jebbor*[2] , *Ahmed El Abassi*[2], and *Seddik Bri*[3]

[1] Faculty of Applied Sciences, Ibno Zohr University, Ait Melloul Agadir 80000, Morocco
[2] Electronic, Instrumentation and Intelligent Systems team, ER2TI Laboratory, Department of Physics Faculty of Sciences and Technics, Moulay Ismail University of Meknes, Errachidia 52000, Morocco
[3] MIN, Electrical Engineering Department, ESTM, Moulay Ismail University of Meknes, Errachidia 52000, Morocco

Abstract. The metamaterial absorber's new conception and simulation are presented in this paper. Two peaks of 97% and 99,8% are respectively shown by the absorption spectrum at the resonance frequencies 12,5 GHz and 14,5 GHz. Absorptivity is greater than 80% in the 6 GHz – 16 GHz frequency band and is sensitive to both polarization and incidence's angles. Clearly this structure provides absorption more than 90% in the range frequency 11,9 GHz -15 GHz. The simulations' results have revealed that the absorption characteristics can be controlled either by adding resistors to the metallic pattern or by changing its geometric or physical parameters. The proposed structure's impedance is approximately equal to that of the free space at the resonance frequencies, which explains the perfect absorption's obtention at these frequencies. A numerical comparison of our absorber with the four broadband perfect absorbers reported in the literature, leads to satisfactory Conclusion. This designed metamaterial absorber can be applied to antennas to improve their directivities.

1 Introduction

Metamaterial absorbers have attractive features unlike conventional wave absorbers [1]. In this study, a perfect metamaterial absorber was identified by adjusting its effective permittivity and permeability to minimize transmittance and reflection at the resonance frequency. Both transmission and reflection are minimized by achieving a metamaterial absorber's input impedance equal to that of the free space and significant losses due to the imaginary parts of its effective parameters. Different single, double, triple and multi-band absorbers were then designed with features namely insensitivity to polarization and incidence's wide angle [2-7]. Research have also been carried out on many absorptions band widening methods such as single-layer planar absorber [8], broadband absorber based on lumped resistors [9] and multi-layer absorber [10]. Compared to conventional millimeter wave absorbers that are physically thick and have limited frequency performance, metamaterial absorbers can be used to suppress microwaves reflected by metallic structures due not only to their ultra-high nature thin but also to their quasi-unit absorptivity and their increased efficiency [11-12].
In this work, we have proposed a metamaterial absorber which unit cell is composed of a resonator formed by two concentric copper ellipses with a rotation of 30^0, and a copper plate located respectively on the surface and at the bottom of the FR4 dielectric substrate with loss. The structural parameters of our absorber are optimized and have a broadband absorption response covering the frequencies range 4 GH - 18GHz, with the absorptivity of more than 80%. The electric field distribution and the impedance adaptation theory have been used to understand the absorption mechanism. We have demonstrated that the proposed absorber's impedance is almost equal to that of the free space for 12,5 GHz and 14.5 GHz resonance frequencies, which have respectively a greater absorptivity than 97% and 99.8%. In addition, the absorber is a single layer structure.

2 Design of the proposed absorber

The simulated structure is illustrated in Fig. 1, and optimal structural parameters are displayed in table 1.
As shown in Fig. 1, copper was plated on the upper and lower surfaces of the FR4 substrate of thickness $\mathbf{a_z}$. The upper surface consists of two ellipses. Both the large and the small axis of the inner ellipse are **a** and **b**, respectively. The geometric center coincides with the unit cell's center and the rotation's angle of the width's two ellipses is 30^o. The FR4 substrate with a dielectric constant of 4.3, a loss

* Corresponding author: r.chaynane@uiz.ac.ma

coefficient of 0.025, has length $\mathbf{a_x}$, $\mathbf{a_y}$ width and $\mathbf{a_z}$ thickness. The metallic pattern is loaded with four lumped resistors.

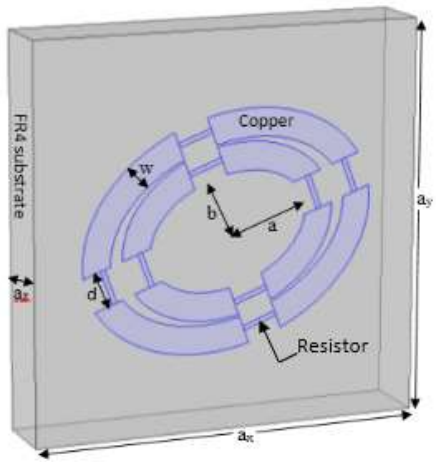

Fig. 1. Structure of metamaterial unit cell

Table 1. Optimized values of the geometric and the unit cell's physical parameters

w	1.2 mm
a	3.5 mm
b	2.3 mm
d	1.5 mm
a_x	16.6 mm
a_y	16.6 mm
a_z	3 mm
R	180 Ohm
FR4 substrate thickness	3 mm
Thickness of copper patterns	30 µm
Copper conductance	5.96 107 S/m
Relative permittivity of the substrate	4.3(1.0 + j0.025)
Relative permeability of the substrate	1.0.(1.0 + j0.0)
Dimensions of the unit cell	$a_x \times a_y \times a_z$

Periodic boundary conditions have been used for the x and y directions, so that the simulated metamaterial absorber extends to infinity on the **xy** plane. The excitation wave propagates in the **z**-direction. We simulated the proposed absorber's different characteristic parameters using the finite element method. The absorption can be calculated via equation:

$$A(\omega) = 1 - |S_{11}|^2.$$

3 Results and discussions

3.1. Resistors' effect on the absorptivity

Fig.2 reveals the proposed structure's absorption responses under normal incidence for both polarization TE and TM, without and with load resistances. The metal motif's absorption performance with four resistances is significantly much better compared to the one without resistances. Motif with lumped resistors covers the entire frequency range 7 GHz – 16,25 GHz with an absorptivity of more than 80%. As far as the frequency band 11,9 GHz – 15 GHz is concerned, the proposed absorber provides an absorptivity exceeding 90% corresponding to bandwidth of 3,1 GHz. There are two separate absorption peaks at 12,5 GHz and 14,5 GHz corresponding to a maximum absorptivity of 97% and 99,8%, respectively.

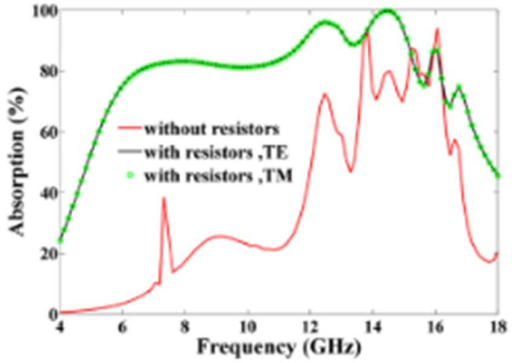

Fig. 2. Absorption spectra of the designed MMA structure

3.2 Polarization and incidence angles' effects on absorptivity.

The polarization angle's effect on the proposed structure's absorptivity has also been studied for the value of the angle ϕ varying between 0° and 40° under normal incidence, as indicated in Fig. 3. Absorption is insensitive to the polarization's angle in the frequency band 4 GHz – 10 GHz, Fig. 3a, however decreases gradually in the frequency ranges 10 GHz – 15 GHz and 16 GHz – 18 GHz with increasing angle ϕ. While the absorptivity increases gradually in the frequency band 15 GHz – 16 GHz, in polarization TE. In polarization TM, fig. 3b, the absorption is very sensitive to the polarization's angle. This sensitivity to the polarization's angle is solicited in the radar imaging field [13].

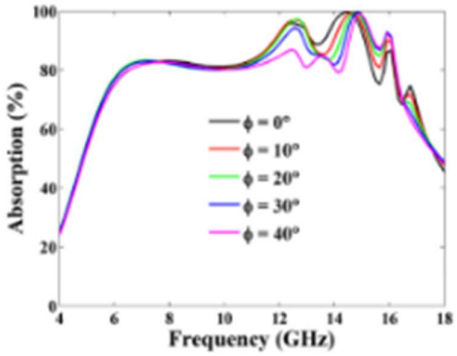

(a) TE mode

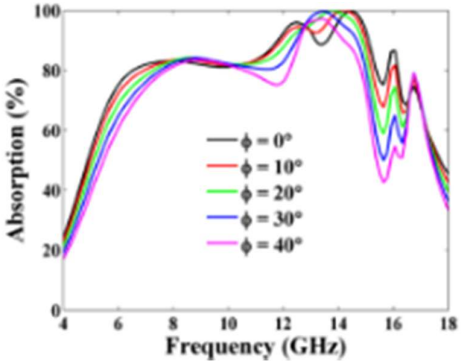

(b) TM mode

Fig. 3. Effect of the polarization angle on the absorption

The proposed structure is then studied for different oblique incidence angles from 0° to 30°, in polarization TE, as displayed in Fig. 4. The sensitivity of the structure's absorptivity to the oblique incidence's angle is observed. The absorptivity is greater than 80% in frequency band 6 GHz -16 GHz for $0° < \theta < 30°$.

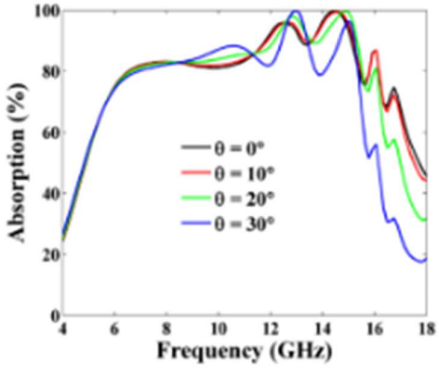

Fig. 4. The incidence angle's effect on the absorption

3.3 Absorption's Mechanism.

Fig. 5 illuminates the electric field's distribution of the proposed absorber for the two resonance frequencies 12,5 GHz and 14,5 GHz. The images show an intense electric field's presence at the ellipses' outer and inner edges. This explains why the elliptic resonator is mainly responsible for producing absorption peaks at these resonance frequencies.

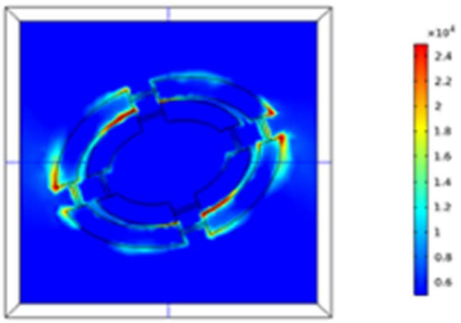

(a) f = 12,5 GHz

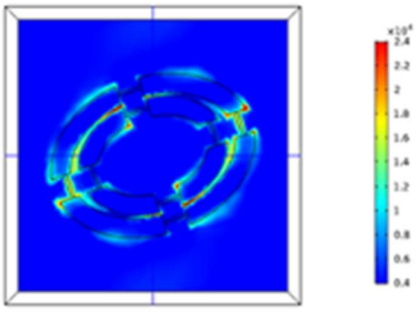

(b) f = 14,5 GHz

Fig. 5. Electric field's Distribution at resonance frequencies

Effective electromagnetic parameters are extracted to better understand the absorption's physical mechanism of the proposed metamaterial structure. These parameters are calculated from electrical and magnetic susceptibility as displayed in the equations [14-15]:

$$\chi_{es} = \frac{2jS_{11}-1}{k_0 S_{11}+1} \quad (1)$$

$$\chi_{ms} = \frac{2jS_{11}+1}{k_0 S_{11}-1} \quad (2)$$

$$\epsilon_{eff} = 1 + \frac{d}{\chi_{es}} \quad (3)$$

$$\mu_{eff} = 1 + \frac{d}{\chi_{ms}} \quad (4)$$

$$Z = \sqrt{\frac{(1+S_{11})^2 - S_{21}^2}{(1-S_{11})^2 - S_{21}^2}} = \frac{1+S_{11}}{1-S_{11}} \quad (5)$$

Where k_0 is the free space's wave number, and d is the distance to be travelled by the incident wave. This method does not involve the extraction of the transmission coefficient S_{21} and more robust than the S-parameters inversion method [16].

According to the impedance adaptation's theory, the perfect absorption is achieved when permittivity and permeability are equal. The real and imaginary parts of the electromagnetic properties are shown in Fig. 6 and 7. Permittivity and permeability are close to the resonance frequencies 12,5 GHz and 14,5 GHz, indicating that the proposed absorber's impedance is approximately equal to the free space. The permittivity and permeability real parts are almost equal as well as the imaginary parts, as shown in Fig. 6 and 7. The proposed absorber minimizes the reflection and with a large electrical loss tangent and a large magnetic loss tangent at the same time, permitting to have an almost perfect absorption mainly at the resonance frequencies 12,5 GHz and 14,5 GHz.

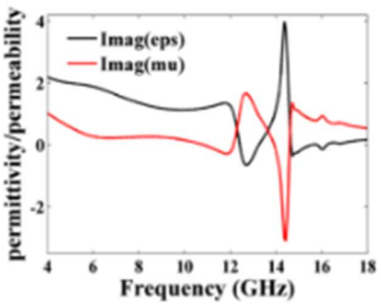

Fig. 6. Permittivity and permeability's imaginary parts

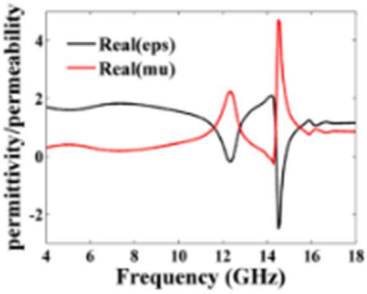

Fig. 7. Permittivity and permeability's real parts.

3.3 Comparison

This section compares, as presented in Fig. 8, the proposed absorber with the perfect absorbers reported in Ref [17-20]. In the C-band, our absorber has the best absorptivity performance except for the perfect absorber in Ref [17], unlike in the X-band. In the frequency range 12 GHz – 15 GHz, the proposed absorber can be considered a perfect one. Regarding the different absorbers' designs used in this numerical comparison, only our absorber is simple, the others present a manufacturing complexity.

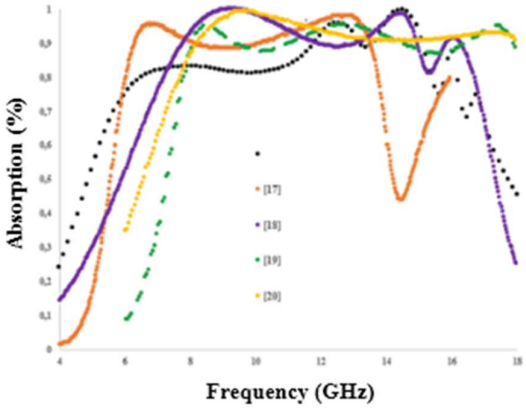

Fig. 8. Comparison of our simulated model and simulated absorption [17-20]

4 Conclusion

To wrap up, the idea of having a broadband absorption response using the three layers' combination was adopted. The proposed metamaterial absorber is composed of two ellipses with four localized resistors, an FR4 material and a metallic mass. The thickness metallic mass is designed to be greater than its skin thickness in the studied frequency ranges, in order not to transmit through any electromagnetic radiation. The designed structure's characterization is carried out by a software based on Finite Element method (FE). The structure provides an absorption value greater than 80% over a frequency wide-band (C, X and Ku) for commonly used wireless communications. Retrieved effective parameters reveals that the permittivity and permeability are almost equal at the resonance frequencies 12,5 GHz and 14,5 GHz, so that the structure behaves as a perfect absorber at these resonance frequencies with absorptivity greater than 97% and 99,8%, respectively. The absorption mechanism was also studied by analyzing the electric field distribution at these resonances' frequencies.

References

1. P. Ranjan, C. Brade, A. Choubey, R. Sinha, S. K. Mahto, SN Applied Sciences **2**,1061 (2020).
2. B. Wang, T. Koschny, C. M. Soukoulis, Phys. Rev. B 80(**3**), 0331081-0331083 (2009).
3. M. Li, H. L. Yang, X. W. Hou, Y. Tian, D. Y. Hou, PIERS **108**, 37-49 (2010).
4. X. J. He, Y. Wang, T. L. Gui, Q. Wu, PIERS **115**, 381-397 (2011).
5. B. R. Bian, S. B. Liu, S. Y. Wang, X. K. Kong, H. F. Zhang, B. Ma, H. Yang, J. App. Phys 114(**19**), 194511 (2013).
6. T. M. Kollatou, A. I. Dimitriadis, S. D. Assimonis, N. V. Kantartzis, C. S. Antonopoulos, PIERS **136**, 579-594 (2013).
7. K. Ozden, O. M. Yucedag, A. Ozer, H. Bayrak, H. Kocer, H., *Metamaterial based dual-band and polarization independent RF absorber*, in International Conference on electrical and Electronics Engineering, ELECO, November 2015, Bursa, Turkey (2015).
8. S. Gu, B. Su, X. Zhao, J. App. Phys 114(**16**), 163702 (2013).
9. S. J. Li, J. Gao, X. Y. Cao, W. Q. Li, Z. Zhang, D. Zhang, J. App. Phys 116(**4**), 043710 (2014).
10. M. R. Soheilifarand, R. A. Sadeghzadeh, AEU-I. J. E. C 69(**1**), 126-132 (2015).
11. C. M. Watts, X. Liu, W. J. Padilla, Advanced Materials 24(**23**), 98-120 (2012).
12. J. Y. Rhee, Y. J. Yoo, K. W. Kim, Y. J. Kim, Y. P. Lee, J. E. W. A 28(**13**), 1541-1580 (2014).
13. G. Sen and al., W. R & Complex Media 29(**1**), 153-161 (2019).
14. S. Bhattacharyya, K. V. Srivastava, J. App. Phys 115(**6**), 4184 (2014).
15. D. R. Smith and al., Phys. Rev E 71(**3**), 036617 (2005).
16. C. L. Holloway, E. F. Kuester, A. Dienstfrey, IEEE Antennas &Wireless Propagation Letters 10(**1**), 1507-1511 (2012).
17. M. Bagmanci, O. Akgol, M. Ozakturk, M. Karaaslan, E. Unal, M. Bakir, Int. J. RF Microw Comput Aided Eng, **21630** (2018).
18. M. Bagmanci, M. Karaaslan, O. altintas, F. Karadag, E. Tetik, M. Bakir, JMPEE 52(**1**), 45-59 (2018).
19. L. Sun, J. Sun, B. Yang, X. Gao, H. Long, Y.Shao, Mat. Re. Express 6(**12**), (2020).
20. K. Chen, X. Luo, G. Ding, J. Zhao, Y. Feng, T. Jiang, EPJ Appl. Metamat 6(**1**), (2019).